

Discrimination of failure criteria with ceramic rings subjected to internal pressure

Patrick Scheunemann*

Institute for Mechanical Engineering Design, Technical University of Hamburg-Harburg, Denickestr. 17, 21073 Hamburg, Germany

Received 30 November 2004; received in revised form 1 June 2005; accepted 10 June 2005

Available online 15 August 2005

Abstract

An experimental procedure for gathering short-time strength data and to discriminate multiaxial failure criteria of ceramics is presented. It uses concentric rings of different diameter ratios which are subjected to internal pressure and allows specimen to have “as-fired”-surfaces. Due to mainly tensional stresses, crack-face friction effects in the material have minor influence on the discrimination of failure criteria. Test series with alumina have been executed and the results are presented.

© 2005 Elsevier Ltd. All rights reserved.

Keywords: Testing; Ring tests; Mechanical properties; Strength

1. Introduction

Strength behaviour and lifetime of ceramic components can be explained by the principles of linear-elastic fracture mechanics. The approach is based on a weakest link theory using a population of planar cracks with random orientation and statistical distributed size.^{2,3,6,7} A component's strength depends on its volume, the distribution of stresses, the assumed type, size and density of flaws and – in case of multiaxial states of stress – a failure criterion. The present paper deals with an experimental procedure which allows the discrimination of failure criteria by using ring-shaped ceramic specimens subjected to internal pressure. The choice of the procedure and the specimens is based on a preceding work about the quantification of the influence of failure criteria on strength prediction.⁹

The failure probability P_f of a ceramic component can be formulated in terms of a Weibull distribution:

$$P_f(\sigma^*) = 1 - \exp \left[- \left(\frac{\sigma^*}{\sigma_0^*} \right)^m \right]. \quad (1)$$

with parameters σ_0^* and m . σ^* is a reference stress which specifies the component's loading, hence σ_0^* denotes a ‘characteristic’ reference stress which leads to a failure rate of 63.2% (characteristic strength).

The prediction of a component's short-time strength distribution (subscript ‘A’) requires a conversion of the characteristic strength obtained from tests with specimens (subscript ‘B’):

$$\sigma_{0,A}^* = \sigma_{0,B}^* \left(\frac{V_{\text{eff},B}}{V_{\text{eff},A}} \right)^{1/m}. \quad (2)$$

This holds under the assumption, that in both cases the same type of flaw population leads to failure, which means that m must be equal for both distributions. The ‘effective volume’ V_{eff} is a variable in which the following effects are summarized: size of the component, its field of stress, the properties of the assumed crack population, and the failure criterion (which is described below). The effective volume is given by

$$V_{\text{eff}} = \frac{1}{4\pi} \int_V \int_0^{2\pi} \int_0^\pi \left[\frac{\sigma_{\text{Ieq}}(\vec{x}, \varphi, \theta)}{\sigma^*} \right]^m \sin \theta \, d\theta \, d\varphi \, dV. \quad (3)$$

$\sigma_{\text{Ieq}}(\vec{x}, \varphi, \theta)$ is a comparative (equivalent) stress for a crack with orientation φ , θ located at \vec{x} under mixed-mode load. It

* Tel.: +49 40 4 28 78 3231; fax: +49 40 4 28 78 2296.

E-mail address: p.scheunemann@web.de.

is calculated using a failure criterion such as the empirical criterion after Richard:⁸

$$\sigma_{I\text{eq}} = \frac{1}{2} \left[\sigma_n + \sqrt{\sigma_n^2 + 4 \left(\alpha_1 \frac{Y_{II}}{Y_I} \tau_{\text{eff}} \right)^2} \right]. \quad (4)$$

Y_I and Y_{II} are factors describing the geometry of the cracks. The parameter α_1 allows the adaption to test results and sets the sensitivity against shearing stress, respectively mode II and mode III loading^a, on the crack. Due to this adjustability, the criterion after Richard was used to define indicators in the preceding paper.⁹ σ_n is the stress normal to the crack plane. In case of negative σ_n , the crack is under compressive loading and three assumptions concerning the effect of shear stress (τ_{eff}) are possible: (a) no failure occurs, (b) failure occurs only as a result of shear loading ($\sigma_n = 0$, $\tau_{\text{eff}} = \tau$), (c) failure due to shear loading decreased by frictional force, which leads to the relation of Alpa:¹

$$\tau_{\text{eff}} = \max(0; |\tau| - |\mu \sigma_n|) \quad \text{for } \sigma_n < 0. \quad (5)$$

Surface flaws respectively flaw populations related to the component's surface are considered by an analog approach. In addition to the criterion after Richard the following criteria are used for strength prediction in Section 3:

- mode-I-failure

$$\sigma_{I\text{eq}} = \sigma_n \quad (6)$$

- coplanar energy release rate (ν is the Poisson's ratio)

$$\sigma_{I\text{eq}} = \sqrt{\sigma_n^2 + \tau_{\text{eff}}^2 \left[\left(\frac{Y_{II}}{Y_I} \right)^2 + \frac{1}{1-\nu} \left(\frac{Y_{III}}{Y_I} \right)^2 \right]} \quad (7)$$

- maximum noncoplanar energy release rate

$$\sigma_{I\text{eq}} = \sqrt[4]{\sigma_n^4 + 6\sigma_n^2\tau_{\text{eff}}^2 \left(\frac{Y_{II}}{Y_I} \right)^2 + \tau_{\text{eff}}^4 \left(\frac{Y_{II}}{Y_I} \right)^4} \quad (8)$$

- maximum hoop stress factor

$$\sigma_{I\text{eq}} = \frac{\sqrt{8[2\sigma_n + 6\sqrt{\sigma_n^2 + 8((Y_{II}/Y_I)\tau_{\text{eff}})^2}](Y_{II}/Y_I)\tau_{\text{eff}}^3}}{[\sigma_n^2 + 12((Y_{II}/Y_I)\tau_{\text{eff}})^2 - \sigma_n\sqrt{\sigma_n^2 + 8((Y_{II}/Y_I)\tau_{\text{eff}})^2}]^{1.5}} \quad (9)$$

When used for the calculation of the effective volume (Eq. (3)), the maximum value of $\sigma_{I\text{eq}}$ along the crack front has to be chosen. For circular cracks and the criteria shown here, this is where shear stress is perpendicular to the crack front.

The effective volume, as a variable which depends on the choice of the failure criterion, can be used to define two sensitivity indicators I_{F1} and I_{F2} .⁹ They quantify the effect of failure criteria on strength prediction and allow distinction of the particular influences of the multiaxial failure criterion and of an additional criterion for the cracks' behaviour under

compressive load. The indicators are defined by two values of effective volume, which are calculated for the field of stress of a component or specimen for different parameters α_1 and μ of the criteria after Richard and Alpa. The first indicator I_{F1} is a measure for the sensitivity of a component's strength prediction against changing the failure criterion. The second indicator I_{F2} describes the sensitivity against changing the reduction of shear stress on a crack due to frictional effects under compressive crack loading (see Eq. (5)). Both indicators do not depend on the absolute level of stresses and stay constant upon rescaling of the component. A value of zero indicates that there is no effect of the choice of failure criterion, increasing values indicate an increasing effect.

To extract an applicable failure criterion for a specific material, test results obtained from a test with low I_{F1} should be compared with results from a test with high I_{F1} . On the other hand the I_{F2} -values should be as low as possible, since a high value indicates that the failure is affected by compressive stresses. This would lead to a mixed influence of the failure criterion itself and of frictional effects and is therefore not wanted. Numerical values for spatial constant states of stress, for typical experimental setups and for real components have been calculated. Due to this results, testing of ring-shaped specimens with different diameter ratios under internal pressure was found to be a promising approach to cover a medium range of I_{F1} with low I_{F2} .

2. Specimens and experimental setup

Test series on two different types of ring-shaped specimens (Fig. 1) have been carried out on alumina (99.7% Al_2O_3). The aim was to gather short-time strength data and to determine a failure criterion for the strength prediction of components made of alumina in hydrostatic machines. Both types of rings have been produced by a commercial manufacturer and show as-fired conditions on inner and outer surface (R_z between 2.4 and 4.8 μm) and polished planar faces ($R_z = 0.65 \mu\text{m}$). Due to the different diameter ratios the state of stress on the inner surface (location of highest tensile stress) reads for type-A:

$$\frac{\sigma_2}{\sigma_1} = -0.18 \quad \text{and} \quad \frac{\sigma_3}{\sigma_1} = -0.20 \quad \text{with } \sigma_1 = 4.98p \quad (10)$$

and for type-B:

$$\frac{\sigma_2}{\sigma_1} = \frac{\sigma_3}{\sigma_1} = -0.54 \quad \text{with } \sigma_1 = 1.85p, \quad (11)$$

where p denotes the applied internal pressure. σ_1 is the tensile hoop stress, σ_3 is the radial compressive stress due to internal pressure, and σ_2 arises from fluid pressure gradients across the planar faces. Their computation is described below.

Test on selected samples of type-A-rings showed a low level of concentricity deviations. Stress corrections due to

^a Mode I: tension normal to crack plane, mode II: shear loading normal to crack front, mode III: shear loading in direction of crack front.

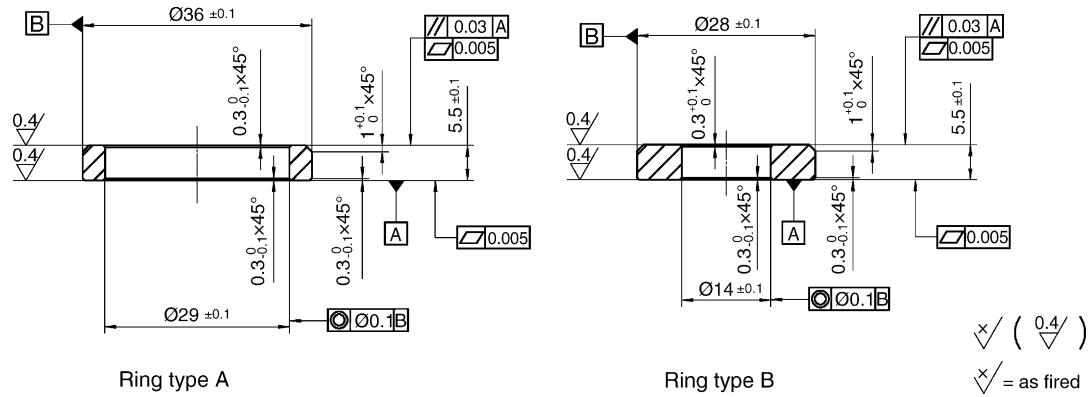


Fig. 1. Ring-shaped specimens for internal pressure testing.

these deviations stayed below 0.2% and have been neglected. Deviations of type-B-rings were found to show very low influence on stresses and have also been neglected.

The corresponding test stand feeds a constant volumetric flow to the interior of the specimen, which escapes through gaps between ring and pressure-plate respectively fixation-plate (Fig. 2). The internal pressure is controlled by the force F as it determines the height and the choking effect of the gaps. A slightly asymmetric design of the specimens (one outer chamfer increased) was chosen to reduce risk of oscillation of the specimen with still a second (but very narrow) gap existing, which reduces influence of friction. Both types of specimens can be used in the same test stand without the need for modifications. Load induction by fluid allows one to use inner and outer surfaces of the rings in as-fired conditions as it does not lead to local gradients of contact stresses due to bumpiness when inducing load via rigid bodies.

Due to the choking effect of the gap flow, the oil temperature rises from the inner to the outer portions of the specimen. This leads to thermal stresses, which have to be taken into account. In addition, there is a mutual influence of the fluid pressure gradients in the gaps, the temperature-dependency of the fluid viscosity and the elastic deformation of the specimen and the fixation plates. For a computation of these effects a co-simulation of the gap flow, the transient temperature field and the elastic deformations was executed for each ring type (see¹⁰ for a detailed description). Stresses

in Eqs. (10) and (11) already include thermal stresses and compressive stresses due to the fluid pressure gradients for alumina. The surrounding medium used in the tests was mineral oil for fluid power applications (Shell Tellus 68). Fig. 3 shows the test station with the pressure control valve which controls the force F , produced by the hydraulic cylinder. The test rig can produce up to 1000 bar in continuous operation and up to 1500 bar in short-time tests.

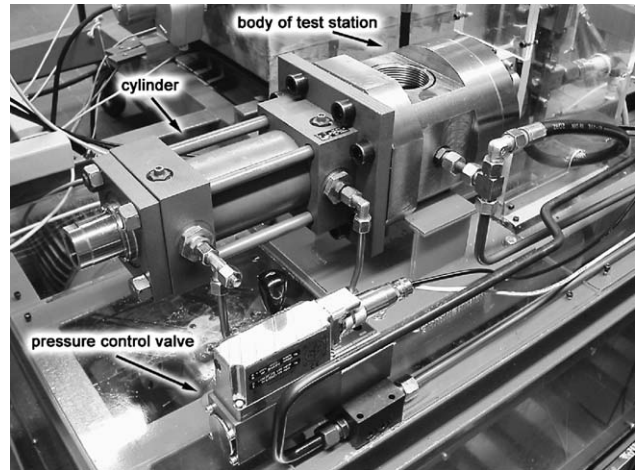


Fig. 3. Test rig.

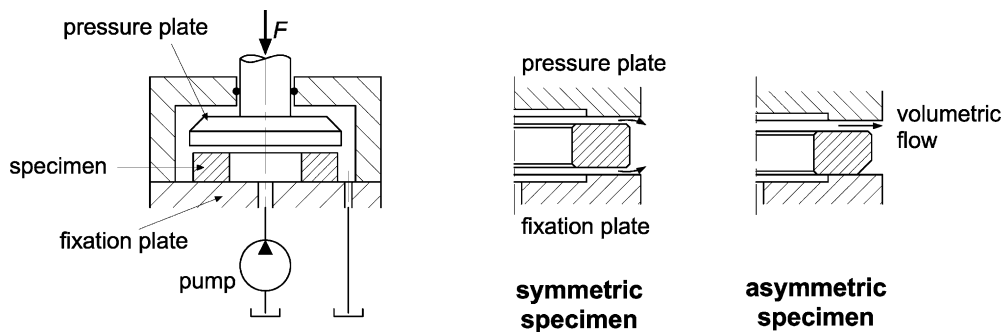


Fig. 2. Principle of internal pressure testing (left); gap flow with symmetric and asymmetric specimen.

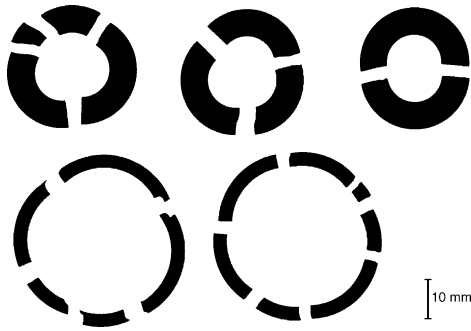


Fig. 4. Typical examples of bursted rings.

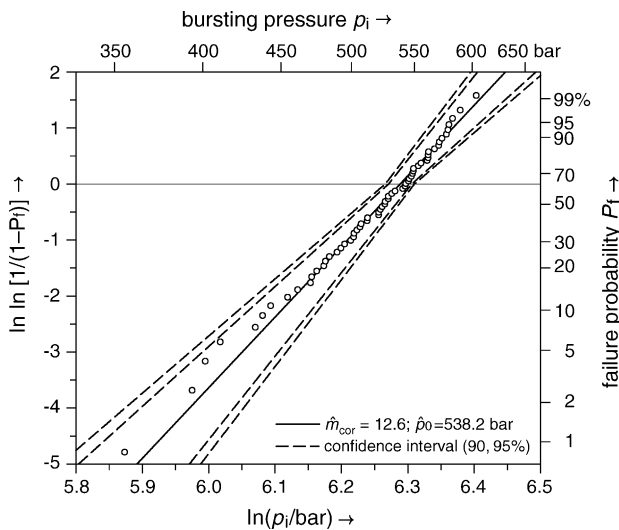


Fig. 5. Weibull plot of the test results, Al₂O₃, ring type-A.

3. Results

Two test series have been executed: the first one on 61 rings of type-A, the second one on 22 rings of type-B. In both cases the temperature of the surrounding medium was 40 °C. The climb rates of the internal pressure used for short-time strength testing were 3800 bar/s on type-A-rings and 6900 bar/s on type-B-rings, which leads to climb rates of 1750 MPa/s (type-A) respectively 1100 MPa/s (type-B) for tensile stresses on inner surface of the rings.

Fig. 4 shows typical examples of bursted rings. Weibull parameters of the distribution of bursting pressures has been determined according to the European Prestandard ENV 843-5.⁵ Figs. 5 and 6 and Table 1 summarize the test results.

To find out, which of the failure criteria is suitable for the prediction of a component's strength behaviour, the characteristic strength (here: bursting pressure) of type-B-rings was calculated from the test results of type-A-rings using Eq. (2). V_{eff} and A_{eff} were computed from FEM-results using a self-coded software. This was done for volume flaws (circular cracks)^b and surface flaws (semicircular cracks), and for

^b $Y_{\text{II}}/Y_{\text{I}} = 1.117$ and $Y_{\text{III}}/Y_{\text{I}} = 0$ at the location of the crack front with maximum equivalent stress σ_{Ieq} .

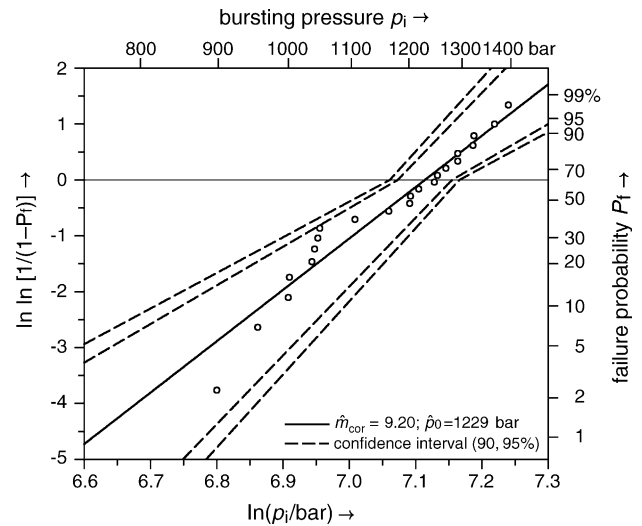


Fig. 6. Weibull plot of the test results, Al₂O₃, ring type-B.

different failure criteria (Eqs. (4) and (6)–(9)). In case of the criterion after Richard (Eq. (4)) the parameter α_1 was varied for best fitting. In all cases compressive stresses were incorporated by using the criterion after Alpa (Eq. (5)) with $\mu = 0$ and $\mu \rightarrow \infty$, the latter means that there is no failure due to shear stress under compressive stress on crack plane. The Weibull-modulus used for the calculation was $m = 12.6$, in case of prediction using effective surfaces, only surfaces in as-fired-conditions have been used (inner and outer surface).

Then the calculated strength of type-B-rings was compared with the observed strength from the test series. The 90% confidence intervals were determined to take account of the statistical uncertainty of the results. Fig. 7 summarizes the different predictions. It shows that failure criteria with low sensitivity against shear stress (mode-I-failure, criterion after Richard with low α_1) generate too high bursting pressure predictions. Criteria with high shearing sensitivity generate better predictions, but to fit the results a unusual high value of $\alpha_1 \geq 3$ is needed. Predictions which are using the effective surface need less α_1 -values for fitting. Due to the coarse surface and the fact that the highest tensile stress can be found on the inner surface of the rings, it is most likely that failure is triggered by surface flaws. Because of the number of fragments respectively fracture surfaces (see Fig. 4) an exact location of fracture origins was not possible.

A variation of the friction-parameter μ in the criterion after Alpa does not change the prediction significantly (left and right values of the displayed pairs), which was a demand for the choice of the test procedure.

The non-applicability of common criteria (Eqs. (6)–(9)) and of the criterion after Richard with a parameter-range of $0.5 \leq \alpha_1 \leq 1.3$ on alumina was also reported by Schöpke.¹¹ His experiments were also carried out on specimens with as-fired-surfaces and with mineral oil as surrounding medium. Whereas Brückner-Foitt et al.⁴ found shear-insensitive criteria to be applicable for alumina by comparing tests with

Table 1
Weibull parameters and confidence intervals

Value	Unit	Type-A-rings	Type-B-rings
Number of specimens	–	61	22
Weibull modulus m	–	12.62	9.20
Characteristic bursting pressure p_0	Bar	538.2	1229
Confidence interval (95%)			
Weibull modulus	–	[10.21,15.50]	[6.38,13.08]
Busting pressure	Bar	[526.2,550.2]	[1165,1295]
Confidence interval (90%)			
Weibull modulus	–	[10.70,14.92]	[6.91,12.31]
Busting pressure	Bar	[528.9,547.7]	[1180,1281]

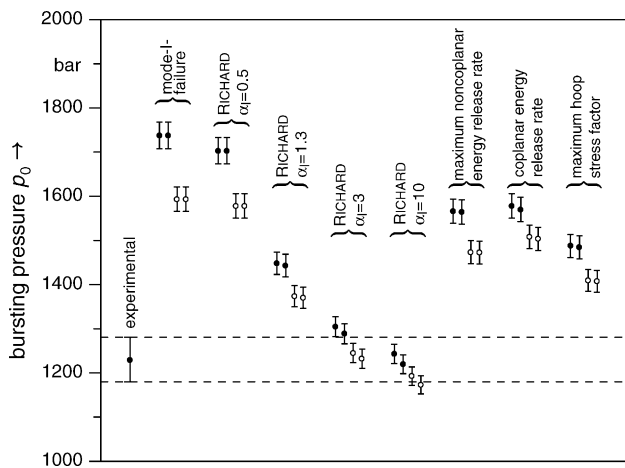


Fig. 7. Comparison of experimental and predicted characteristic bursting pressure of type-B-rings, using different failure criteria; calculation with effective volume (●) respectively effective surface (○); left value of pairs: $\mu \rightarrow \infty$, right: $\mu = 0$ in the criterion after Alpa.

mainly tensional stresses with Brazilian disk tests, which shows mainly compressive stresses. In this case a superimposed effect of frictional forces between the surfaces of the cracks occurs, which may explain the different results. Since the manufacturing process of ceramic components has a large influence on their strength properties, the results may be very sensitive against differences between the two specimens. This underlines the necessity of careful production of both specimen types. Though type-A- and type-B-rings were made of the same material with equivalent processing, some uncertainties are still remaining, e.g. residual stress due to the sintering process. Further test series with different materials and different manufacture processes are necessary.

4. Conclusion

Testing concentric rings of different diameter ratios under internal pressure was found to be a good approach to prove the applicability of multiaxial failure criteria for ceramics. Due to mainly tensional stresses ($\sigma_1 > |\sigma_3|$) frictional effects between cracks' surfaces have very low influence on the results of the determination of applicable failure criteria. Load

induction by fluid allows one to use specimens with coarse inner and outer surfaces, which is of interest for strength prediction of ceramic components with surfaces which are left in as-fired conditions due to cost reduction. Bursting tests of two types of rings with as-fired surfaces have been executed on alumina; experimental results have been compared with strength predictions based on different failure criteria. The results show the need of criteria with high sensitivity against shear stress to fit experiment and prediction. This was also observed Schöpke,¹¹ while other authors found shear-insensitive criteria being applicable.⁴ One possible explanation is the different amount of compressive stresses, which occur in the different experimental procedures.

References

- Alpa, G., On a statistical approach to brittle rupture for multiaxial states of stress. *Eng. Fracture Mech.*, 1984, **19**(5),881–901.
- Batdorf, S.B. and Crose, J.G., A statistical theory for the fracture of brittle structures subjected to nonuniform polyaxial stresses. *J. Appl. Mech.*, 1974, **41**, 459–464.
- Batdorf, S.B. and Heinisch, H.L., Weakest link theory reformulated for arbitrary fracture criterion. *J. Am. Ceram. Soc.*, 1978, **61**, 355–358.
- Brückner-Foit, A., Fett, T., Munz, D. and Schirmer, K., Discrimination of multiaxiality criteria with the Brazilian Disc Test. *J. Eur. Ceram. Soc.*, 1997, **17**, 689–696.
- European Committee for Standardization (CEN): European Prestandard ENV 843-5, *Monolithic ceramics—mechanical tests at room temperature, Part 5: Statistical analysis*.
- Munz, D. and Fett, T., *Mechanisches Verhalten keramischer Werkstoffe*. Springer-Verlag, Berlin, 1989, pp. 83–95.
- Munz, D. and Fett, T., *Ceramics: Mechanical Properties, Failure Behaviour, Materials Selection*. Springer-Verlag, Berlin, 1999, pp. 137–158.
- Richard, H.-A., Bruchvorhersagen bei überlagerter Normal- und Schubbeanspruchung von Rissen. In *VDI-Forschungsheft Bd. 631*. VDI-Verlag, Düsseldorf, 1985, pp. 49–53.
- Scheunemann, P., The influence of failure criteria on strength prediction of ceramic components. *J. Eur. Ceram. Soc.*, 2004, **24**, 2181–2186.
- Scheunemann, P., *Verfahren und Vorrichtungen zur Bestimmung von Werkstoffdaten für die Lebensdauerabschätzung keramischer Bauteile*. Cuvillier Verlag, Göttingen, 2005, pp. 98–115.
- Schöpke, M., Gestaltung, Berechnung und Erprobung hochbeanspruchter Keramikbauteile. *Fortschr. -Ber. VDI-Reihe 1 Nr. 308*. VDI-Verlag, Düsseldorf, 1999, pp. 79–81.